Solid State Lithium Cyanocobaltates with a High Capacity for Reversible Dioxygen Binding: Synthesis, Reactivity, and Structures

Dorai Ramprasad,* Guido P. Pez, Brian H. Toby,† Thomas J. Markley, and Ronald M. Pearlstein

Contribution from the Corporate Science and Technology and Corporate Analytical Technology Centers, Air Products and Chemicals, Inc., 7201 Hamilton Boulevard, Allentown, Pennsylvania 18195-1501

Received May 1, 1995[⊗]

Abstract: Lithium pentacyanocobaltate coordination polymers with the formulas $Li_3[Co(CN)_5]\cdot 4DMF$ (**1**, DMF = *N,N*-dimethylformamide) and $Li_3[Co(CN)_5]\cdot 2DMF$ (**2**) have been synthesized and structurally characterized. Both compounds react reversibly with O_2, forming 1:1 superoxo complexes. Compound **2** reacts more rapidly and has the highest reported capacity for a solid O_2 carrier (55 std cm^3/g). In contrast to previously reported dioxygen complexes of cyanocobaltates, the novel ability of **1** and **2** to react reversibly with O_2 is made possible by the interaction of Li cations with the nucleophilic N atoms of the cyanide ligands. This interaction effectively reduces the basicity of the cyanide ligands, decreasing the net electron density on Co(2+) and hence weakening the charge-transfer interaction with O_2. The structure of **1** was determined from single-crystal X-ray diffraction measurements. It crystallizes in the triclinic space group $P\bar{1}$ (no. 2) with $a = 11.568(7)$ Å, $b = 14.244(3)$ Å, $c = 8.118(3)$ Å, $\alpha = 97.44(2)°$, $\beta = 103.00(4)°$, $\gamma = 94.64(3)°$, and $Z = 2$. Monocrystals of **2** suitable for X-ray structural analysis could not be grown, but the structure was solved *ab initio* from synchrotron powder diffraction data by using a simulated-annealing technique. The monoclinic cell of **2** in space group $P2_1/n$ (no. 14) has cell parameters $a = 15.4455(8)$ Å, $b = 8.4216(4)$ Å, $c = 14.1505(8)$ Å, $\beta = 97.780(3)°$, and $Z = 4$.

Introduction

The reactions of metal complexes with molecular oxygen have been studied by many different groups, and several excellent reviews are available on this subject.[1] These studies have been motivated by a desire to mimic biological O_2 carriers and by the potential application of these complexes for the separation and recovery of O_2 from air.[2] Although there are many metal complexes that reversibly bind O_2 in solution, the transposition of this chemistry to the solid state is not trivial.[3] The facile access of O_2 to the reactive metal centers and its ready release upon depressurization or a rise in temperature are key practical requirements.[1c] This work presents a new class of discrete solid complexes that rapidly and reversibly bind O_2, one of which has an exceptionally high pressure-reversible O_2 binding capacity.

The most extensively studied class of solid state metal complexes that reversibly sorb O_2 are the cobalt salcomine[4] complexes in which the O_2 gains access to the cobalt sites, usually with a concomitant phase change.[1b] This phase transformation involves expansion and contraction of the crystallites, and repeated cycling ultimately leads to their physical degradation.[3] In contrast, the cobalt(2+) complexes of the picket fence porphyrin can reversibly bind O_2 without a phase change, presumably because there is sufficient free space within the solid.[5]

Reversible solid state O_2 sorbents have been prepared by the encapsulation of a metal complex within the cage of a synthetic zeolite.[6] Of particular note is the entrapment of cyanocobaltates as ion-paired species: $A_3Co(CN)_5$ and $A_2Co(CN)_4$ ($A = Na^+$, Cs^+) within the supercage of a faujasite zeolite to give reversibly binding complexes.[7] Although a high concentration of cobalt can be incorporated, less than 1% of these atoms are O_2-reactive; hence, low absorption capacities are obtained. The compounds presented here are also cyanocobaltates, but are salts of fixed composition. This allows virtually all of the Co centers to be active.

Previous reports indicate that solutions of $[Co(CN)_5]^{3-}$ will react with O_2, but only irreversibly.[8] Heating the isolated solid oxygenated complexes results in their degradation rather than simply in liberation of the bound O_2. Carter et al. more recently described the synthesis of $Li_3Co(CN)_5\cdot 3DMF$ (DMF = *N,N*-dimethylformamide), although they were unable to purify the material in a fixed composition.[9] In this work, we have repeated

* To whom correspondence should be addressed.

† Present address: Reactor Radiation Division, National Institute of Standards and Technology, Gaithersburg, MD 20899. e-mail: BRIAN.TOBY@NIST.GOV.

⊗ Abstract published in *Advance ACS Abstracts*, October 15, 1995.

(1) (a) Jones, R. D.; Summerville, D. A.; Basolo, F. *Chem. Rev.* **1979**, *79*, 139. (b) Niederhoffer, E. C.; Timmons, J. H.; Martell, A. E. *Chem. Rev.* **1984**, *84*, 137. (c) Li, G. Q.; Govind, R. *Ind. Eng. Chem. Res.* **1994**, *33*, 755.

(2) Ramprasad, D.; Gilicinski, A. G.; Markley, T. J.; Pez, G. P. In *The Activation of Dioxygen and Homogeneous Catalytic Oxidation*; Barton, D. H. R., Martell, A. E., Sawyer, D. T., Eds.; Plenum: New York, 1993.

(3) Martell, A. E.; Calvin, M. *Chemistry of the Metal Chelate Compounds*; Prentice-Hall: New York, 1952; p 336.

(4) (a) Calvin, M.; Bailes, R. H.; Wilmarth, W. K. *J. Am. Chem. Soc.* **1946**, *68*, 2254. (b) Barkelew, C. H.; Calvin, M. *J. Am. Chem. Soc.* **1946**, *68*, 2257. (c) Wilmarth, W. K.; Aranoff, S.; Calvin, M. *J. Am. Chem. Soc.* **1946**, *68*, 2263. (d) Calvin, M.; Barkelew, C. H. *J. Am. Chem. Soc.* **1946**, *68*, 2267. (e) Hughes, E. W.; Wilmarth, W. K.; Calvin, M. *J. Am. Chem. Soc.* **1946**, *68*, 2273.

(5) Collman, J. P.; Brauman, J. I.; Doxsee, K. M.; Halbert, T. R.; Hayes, S. E.; Suslick, K. S. *J. Am. Chem. Soc.* **1978**, *100*, 2761.

(6) Imamura, S.; Lunsford, J. H. *Langmuir* **1985**, *1*, 326.

(7) (a) Taylor, R. J.; Drago, R. S.; Hage, J. P. *Inorg. Chem.* **1992**, *31*, 253. (b) Taylor, R. J.; Drago, R. S.; George, J. E. *J. Am. Chem. Soc.* **1989**, *111*, 6610.

(8) (a) White, D. A.; Solodar, A. J.; Baizer, M. M. *Inorg. Chem.* **1972**, *11*, 2160. (b) Kozlov, G. A.; Zhilinskaya, V. V.; Yatsimirskii, K. B. *Teor. Eksp. Khim.* **1981**, *17*, 686.

0002-7863/95/1517-10694$09.00/0

Table 1. Crystallographic Information

	1	2
unit cell setting	triclinic	monoclinic
space group	$P\bar{1}$ (no. 2)	$P2_1/n$ (no. 14)
data collection temperature (K)	153	295
a (Å)	11.568(7)	15.4455(8)
b (Å)	14.244(3)	8.4217(4)
c (Å)	8.118(3)	14.1511(8)
α (deg)	97.44(2)	90
β (deg)	103.00(4)	97.7786(26)
γ (deg)	94.64(3)	90
unit cell volume (Å^3)	1284(1)	1823.81(21)
Z	2	4
unit cell contents	$C_{24}H_{56}Co_2Li_6N_{18}O_8$	$C_{44}H_{56}Co_4Li_{12}N_{28}O_8$
empirical formula	$C_{17}H_{28}CoLi_3N_9O_4$	$C_{11}H_{14}CoLi_3N_7O_2$

their synthesis and have grown single crystals of a polymeric cyanocobaltate with composition $Li_3Co(CN)_5 \cdot 4DMF$ (**1**). Surprisingly, it was found that **1** is capable of reacting with O_2 reversibly at ambient temperatures.

Heating **1** to 160 °C under N_2 results in a new crystalline phase with the composition $Li_3Co(CN)_5 \cdot 2DMF$ (**2**). This new composition was found to reversibly bind O_2 much more rapidly than **1**. The structure of **2** was determined *ab initio* from synchrotron X-ray powder diffraction data and was refined using the Rietveld technique. This is the first example where an organometallic structure of this complexity has been determined by powder diffraction.

Results and Discussion

The reaction of lithium cyanide with cobalt chloride in a 5.2:1 molar ratio in DMF yields a green crystalline precipitate. Carter et al. proposed the formula $Li_3Co(CN)_5 \cdot 3DMF$ but found that the elemental analyses varied from batch to batch.[9] We repeated their synthesis and found that the amount of DMF in the solid can vary between 5 and 3.5 depending upon how the solid is prepared, as described in the Experimental Section. By the slow addition of a $CoCl_2$ solution in DMF to an LiCN solution in the same solvent, single crystals of **1** were grown, and the structural determination confirmed its composition as $Li_3Co(CN)_5 \cdot 4DMF$.

Crystal Structure of $Li_3Co(CN)_5 \cdot 4DMF$ (1). Crystal data and a summary of intensity data collection are tabulated in Tables 1 and 2. Selected bond lengths and angles are listed in Table 3. Compound **1** crystallizes in the triclinic space group $P\bar{1}$ (no. 2). The asymmetric unit shown in Figure 1 is composed of a single empirical formula unit ($C_{17}H_{28}CoLi_3N_9O_4$). The complete unit cell is generated by two of these asymmetric units related by inversion symmetry. The structure of **1** is a complex network of $Co(CN)_5$ moieties linked through its terminal nitrogens by Li atoms into an infinite three-dimensional lattice. The Li atoms coordinate both the $Co(CN)_5$ units and the DMFs, and thus can be considered the "glue" holding the structure together. The $Co(CN)_5^{3-}$ unit is square pyramidal. Its Co−C bonds range from 1.86 to 1.99 Å and are comparable to those in the $(NEt_2(i\text{-}Pr)_2)[Co(CN)_5]$ salt.[10] The coordination geometry about lithium is approximately tetrahedral and is shown schematically in Figure 2. The Li atoms are found in two different pairs, separated by approximately 2.85 Å and bridged by two O-coordinated DMF molecules. One pair of Li atoms, labeled as Li(1), straddles a center of symmetry. The other pair contains Li(2) and Li(3). The Li(1) atoms are coordinated by two terminally bonded CN ligands in addition to two bridging DMF molecules. The Li(3) atom has a similar coordination sphere to Li(1). The Li(2) atom, however, is coordinated by one end on CN ligand and one nonbridging DMF in addition to two bridging DMF molecules.

Table 2. Data Collection and Refinement Information for $Li_3Co(CN)_5 \cdot 4DMF$ (**1**)

diffractometer	Rigaku AFC6R
wavelength (Å)	0.710 69
takeoff angle (deg)	6.0
detector aperture (mm)	6.0 horizontal 6.0 vertical
crystal to detector distance (cm)	40
scan type	$\omega - 2\theta$
scan rate (deg ω/min)	8.0
scan width (deg)	$0.63 + 0.30 \tan\theta$
$2\theta_{max}$ (deg)	40.0
number of measured reflections	total 2540 unique 2379
R_{int}	0.040
corrections	Lorentz polarization
structure solution	direct methods (SHELXS86)
refinement	full-matrix least-squares
function minimized	$\sum w(\|F_o\| - \|F_c\|)^2$
least-squares weights	$4F_o^2/\sigma^2(F_o^2)$
p factor	0.03
anomalous dispersion	all non-hydrogen atoms
number of observed reflections [$I > 3.00\sigma(I)$]	1341
number of variaobes	137
reflection: parameter ratio	9.79
residuals	$R = 0.077$ $R_w = 0.085$
goodness of fit	2.31
maximum in X-ray difference Fourier map (e/Å^3)	1.08
minimum in X-ray difference Fourier map (e/Å^3)	−0.59

Table 3. Selected Bond Distances (Å) and Bond Angles (deg) for **1** (esd in Parentheses)

Co−C(1)	1.92(2)	Co−C(2)	1.86(2)
Co−C(3)	1.91(2)	Co−C(4)	1.91(1)
Co−C(5)	1.99(1)	O(1)−Li(2)	1.91(3)
O(2)−Li(2)	1.98(3)	O(2)−Li(3)	2.08(3)
O(3)−Li(1)	1.99(2)	O(4)−Li(2)	1.98(3)
O(4)−Li(3)	1.99(3)	N1−Li(3)	1.99(3)
N(2)−Li(3)	1.97(3)	N(3)−Li(2)	1.98(3)
N(4)−Li(1)	2.01(3)	N(5)−Li(1)	1.95(3)
Li(1)−Li(1′)	2.85(5)	Li(2)−Li(3)	2.83(4)
C(1)−Co−C(2)	89.1(6)	C(1)−Co−C(3)	171.5(6)
C(1)−Co−C(4)	89.3(6)	C(1)−Co−C(5)	92.5(6)
C(2)−Co−C(3)	88.7(6)	C(2)−Co−C(4)	166.3(6)
C(2)−Co−C(5)	95.1(6)	C(3)−Co−C(4)	90.9(6)
C(3)−Co−C(5)	95.9(6)	C(4)−Co−C(5)	98.6(6)

Oxygenation Studies on $Li_3Co(CN)_5 \cdot 4DMF$ (1).[11] The reactions of O_2 with solutions of the pentacyanocobaltate ion have been studied by several researchers but, with the exception of the above cited zeolite-encapsulated species,[7] the O_2 was always found to be irreversibly bound.[8,12] For example, Wilmarth and co-workers[12] have described the formation of a peroxo dimer in water as represented by

$$2Na_3[Co(CN)_5] + O_2 \rightarrow Na_6[Co(CN)_5(\mu\text{-}O_2)Co(CN)_5]$$

The nonaqueous chemistry of $Co(CN)_5^{3-}$, however, is quite different since 1:1 superoxo adducts $(cat)_3[Co(CN)_5(O_2)]$ (cat

(9) Carter, S. J.; Foxman, B. M.; Stuhl, L. S. *Inorg. Chem.* **1986**, *25*, 2888.

(10) Brown, L. D.; Raymond, K. N. *Inorg. Chem.* **1975**, *14*, 2590.

(11) A sample of this compound used for these experiments was analyzed to be $Li_3Co(CN)_5 \cdot 3.5DMF$. The infrared spectrum and X-ray powder patterns were identical to those of **1**.

(12) Haim, A.; Wilmarth, W. K. *J. Am. Chem. Soc.* **1961**, *83*, 509.

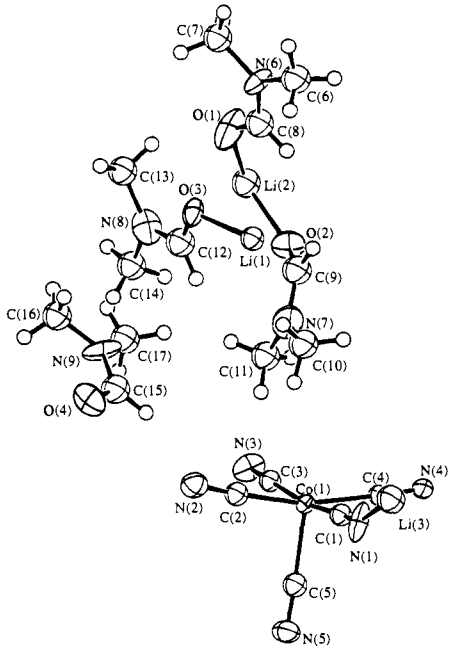

Figure 1. ORTEP diagram of the asymmetric unit of **1** (50% thermal ellipsoids) showing the atom labeling scheme.

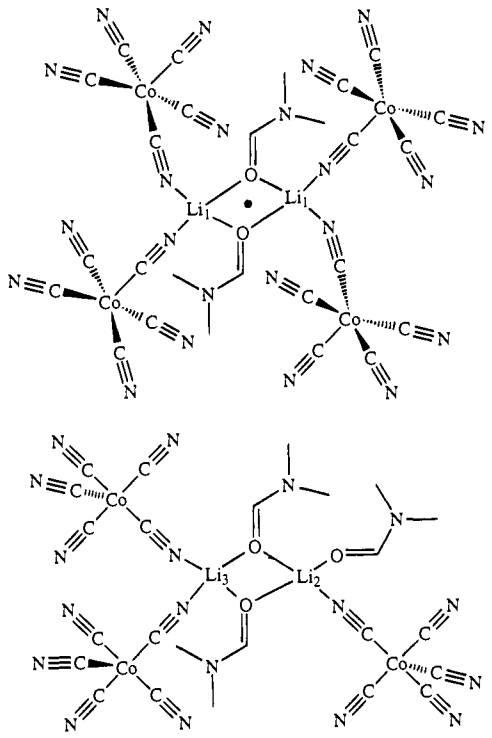

Figure 2. Diagram indicating the coordination environments of Li in **1**.

= NEt_4, $NEt_2(CH_2Ph)_2$, $NMe_2(CH_2Ph)_2$) have been isolated and characterized crystallographically.[13] The tetraalkylammonium cyanocobaltate salt's reaction with O_2 is irreversible at ambient temperature, and an attempt to liberate the bound O_2 from solid $(Bu_4N)_3[Co(CN)_5(O_2)]$ by thermolysis led primarily to the decomposition of the cation, albeit with some O_2 liberation.[8a]

In contrast, the dioxygen reaction of the lithium pentacyanocobaltate, **1**, was found to be reversible. This reactivity is conveniently demonstrated cyclically by observing the changes in the solid's weight when placed under O_2 or N_2. Upon introduction of O_2 to a sample of **1** initially held under N_2, a very slow uptake of 0.877% by weight (0.27 mmol/g corresponding to 0.14 O_2 molecule per Co) was observed over a period of 10 min. On flushing the balance chamber with N_2 for 25 min, a slow desorption of 0.486% (0.15 mmol/g of O_2) was seen. Curve a of Figure 3 shows three such O_2-N_2 cycles, demonstrating that the baseline rises due to incomplete desorption after each cycle. Although the reactivity of **1** with O_2 is slow, approximately 90% of the stoichiometric oxygen capacity per cobalt is reached in 600 min. The chemical nature of the process leading to these weight changes is evidenced by the color of the sample changing from green to red upon oxygenation, along with the appearance of an infrared band at approximately 1130 cm^{-1} which is assigned to a coordinated superoxide vibration.[14] These changes were substantially reversed under N_2. Compound **1** is thus the first example of an unsupported pentacyanocobaltate complex that chemically reacts reversibly with O_2.

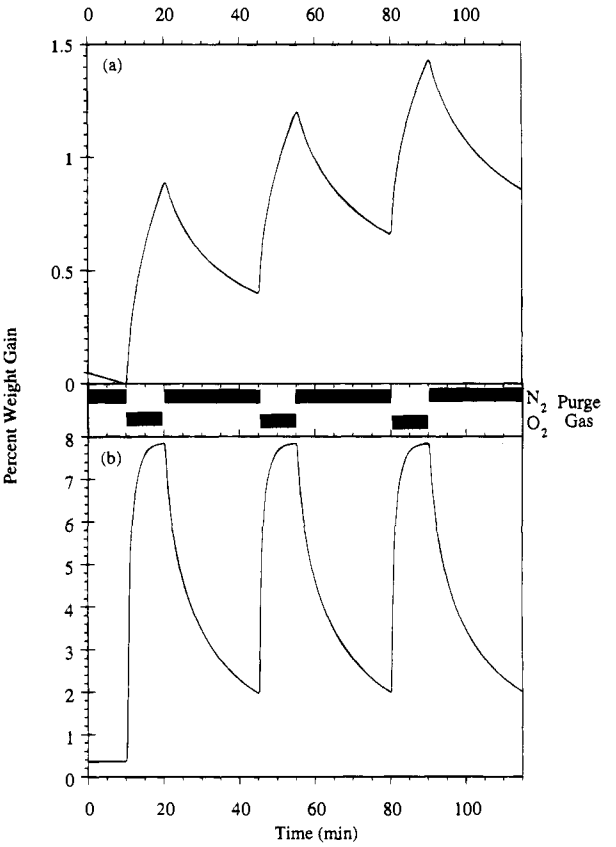

Figure 3. Gravimetric oxygen uptake curves of **1** (a) and **2** (b).

It is hypothesized that this reversibility is made possible by the interaction of the Li cations with the nucleophilic cyanide N atoms, reducing the ligands' ability to donate electron density to cobalt. The DMF molecules coordinate the Li cations and serve to moderate this interaction while also serving as "spacers" for the cobalt centers. The interaction of a cation α^{n+} with a mononuclear hexacyanometalate to form polymeric cyanometalates is well documented and is reflected in the cyanide stretch increasing by 30–70 cm^{-1}.[15] This observation is also consistent for the $Co(CN)_5$ system: ν_{CN} = 2066 cm^{-1} for $(R_4N)_3[Co(CN)_5]$ shifts to 2104 cm^{-1} for **1**.

Synthesis of a New Phase. $Li_3Co(CN)_5 \cdot 2DMF$ (2). Upon heating a sample of **1** to 160 °C, two DMF molecules are lost, leading to the title material, **2**. Its infrared spectrum shows three strong cyanide bands at 2087, 2102, and 2117 cm^{-1} and clearly

(13) Brown, L. D.; Raymond, K. N. *Inorg. Chem.* **1975**, *14*, 2595.

(14) Nakamoto, K. *Coord. Chem. Rev.* **1990**, *100*, 363.

(15) Ludi, A.; Güdel, H. U. *Struct. Bonding (Berlin)* **1973**, *14*, 1.

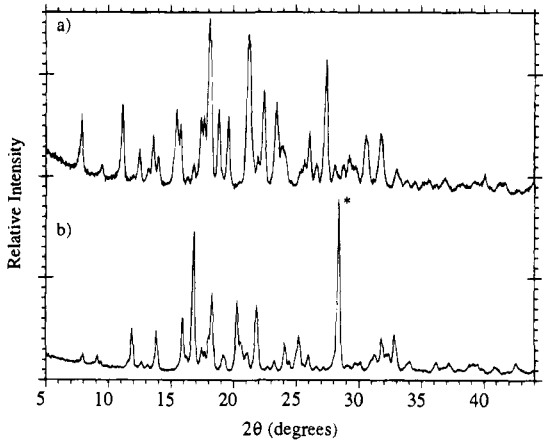

Figure 4. X-ray powder patterns of **1** (a) and **2** (b). A peak from the Si internal standard is indicated by an asterisk.

differentiates it from **1** for which there is a single, strong cyanide band at 2104 cm^{-1}. A clearer distinction between compounds **1** and **2** was obtained from a comparison of their X-ray powder patterns, shown in Figure 4. It becomes apparent that compound **2** has unit cell parameters significantly different from those of its precursor, **1**. The activation process in which ~2 DMF molecules are removed proceeds with retention of crystallinity, as is evidenced by the relatively sharp diffraction peaks.

The following experiments were done in order to see if the $Co(CN)_5^{3-}$ unit was still present in **2**. Stirring a suspension of **2** in O_2-free DMF converted it to **1** without any discernible byproducts. Carter et al. determined the solution spectrum of $Li_3Co(CN)_5$ in DMF and reported bands at 314, 423, 639, and 1055 nm.[9] The low-intensity spin-forbidden band at 639 nm ($^2A_1 \rightarrow {}^4E$) and the stronger band at 1055 nm ($^2A_1 \rightarrow {}^2B_1$) are characteristic of the $Co(CN)_5^{3-}$ system.[16] We find that the solid state UV–vis spectra of both **1** and **2** have these features: a weak band at 624 nm and an intense band in the near-infrared close to the instrumentally imposed cutoff at 900 nm. These results clearly show that the $Co(CN)_5^{3-}$ system is still present in **2**.

Oxygenation Studies on $Li_3Co(CN)_5$·2DMF (2). The new material, **2**, was observed to bind O_2 with significantly faster kinetics and, on a gravimetric basis, with much higher capacity. A sample of **2** was found to absorb ~7% by weight of O_2 (2.3 mmol/g, corresponding to 0.8 O_2 molecule per Co) in 10 min. Upon purging with N_2, the sample released >90% of the sorbed O_2 in 30 min. The O_2–N_2 cycling data for **2** are shown in curve b of Figure 3, which should be contrasted with curve a with respect to the speed of O_2 sorption. When cycled alternately with dry streams of O_2 and N_2, a typical sample of **2** shows a small (~15%) but irreversible loss in activity over 545 cycles (see Figure 5). Exposure to ambient air, however, leads to significant degradation of the sample's reversible O_2 capacity, indicating that the compound is moisture sensitive. Results of volumetric O_2 absorption–desorption isotherm measurements for **2** are shown in Figure 6. These data show that, at 25 °C, **2** has $p_{1/2}(O_2)$ = 26 Torr. At 1 atm partial pressure of O_2 and 25 °C, this compound absorbs ~55 std cm^3/g of O_2 which corresponds to approximately 90% of the stoichiometric capacity per cobalt. This gravimetric oxygen-carrying capacity may be compared with the values <35 std cm^3/g reported for the solid cobalt Schiff base complexes.[4b] It is important to note that, unlike the Schiff base complexes,[4b,c,e] the O_2 absorption of **2** is totally pressure-reversible: there is no hysteresis upon desorption as is demonstrated by the

(16) Caulton, K. G. *Inorg. Chem.* **1968**, *7*, 392.

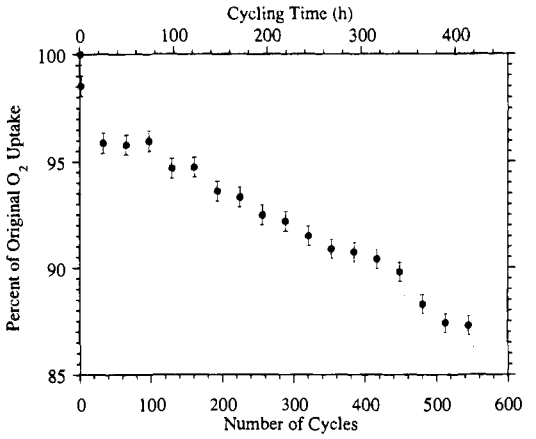

Figure 5. Stability of **2** to repeated O_2–N_2 cycling.

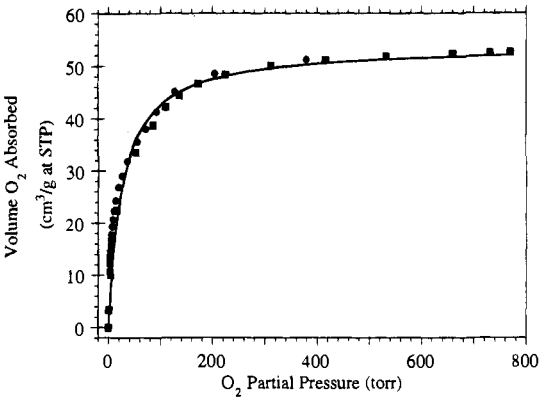

Figure 6. Dioxygen absorption isotherm of **2** at 25 °C. Squares represent absorption data, and circles represent desorption data. The solid line shows a fit to the Langmuir isotherm, $Y = mbp/(1 + bp)$ where Y represents O_2 loading in std cm^3/g of **2**, p is the partial pressure of O_2 in Torr, m (O_2 capacity) = 53.8(8) std cm^3/g, and b (Henry's law constant) = 3.8(3) × 10^{-2} $Torr^{-1}$.

superimposible isotherms measured by either sequentially increasing or decreasing the O_2 partial pressure.

Raman and infrared spectroscopies were used to elucidate the mode of binding of O_2 to **2**. A sample exposed to $^{16}O_2$ showed a band in the Raman spectrum at 1131 cm^{-1} which shifted to 1068 cm^{-1} upon exposure to $^{18}O_2$. A similar result was observed in the infrared spectra. The 1131 cm^{-1} band was assigned to the O–O stretch of a terminally bound "superoxo" group in the complex $[Li_3Co(CN)_5(O_2)]$·2DMF, since this frequency is typical of known cobalt(III) superoxide complexes.[14]

Crystal Structure of $Li_3Co(CN)_5$·2DMF (2). Crystals of **2** suitable for single-crystal diffraction methods could not be obtained. The structure was, however, solved from X-ray powder diffraction data by using a simulated annealing method to position one $Co(CN)_5$ and two DMF molecular units as rigid bodies. Despite use of high-resolution synchrotron data, the large number of atoms in the asymmetric unit necessitated a refinement with constraints. The bond distances and the bond angles within the $Co(CN)_5$ moiety and in the two DMF molecules were fixed at the values obtained for **1**, and were not refined. The crystal data and the asymmetric unit with atom labeling scheme are presented in Table 1 and Figure 7, respectively. Despite the use of a relatively small number of refined parameters, excellent agreement was obtained between the observed and computed diffraction data, as demonstrated by the refinement parameters presented in Table 4.

Compound **2** crystallizes in space group $P2_1/n$; thus, removal of DMF from **1** leads to a significant structural rearrangement

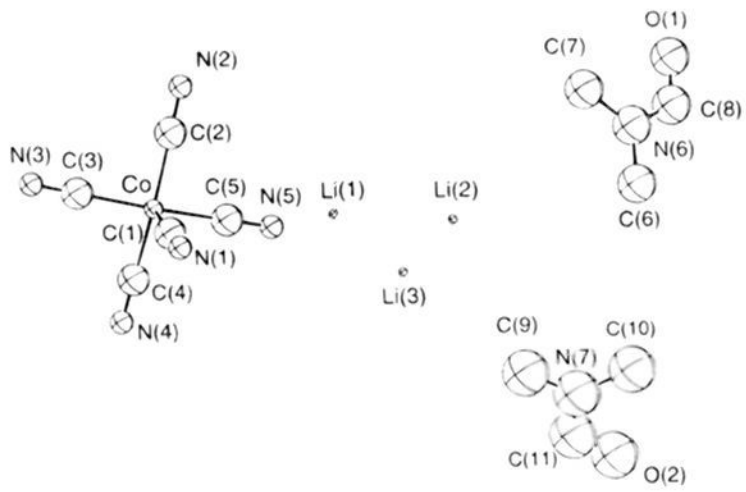

Figure 7. ORTEP diagram of the asymmetric unit of **2** (50% thermal ellipsoids) showing the atom labeling scheme.

Table 4. Data Collection and Refinement Information for $Li_3Co(CN)_5 \cdot 2DMF$ (**2**)

data type	synchrotron X-ray, $\lambda = 1.299\,45$ Å
profile R factor (R_p)	0.0692
weighted profile R factor (R_{wp})	0.0892
expected profile R factor (R_e)	0.0685
reduced χ^2	1.728
Bragg R factor (R_B)	0.0514
range of final difference Fourier map (e/Å^3)	−0.27 to +0.29
2θ range (deg)	6−50
number of reflections	531
profile function	pseudo-Voigt
background function	20-coefficient Chebyshev polynomial

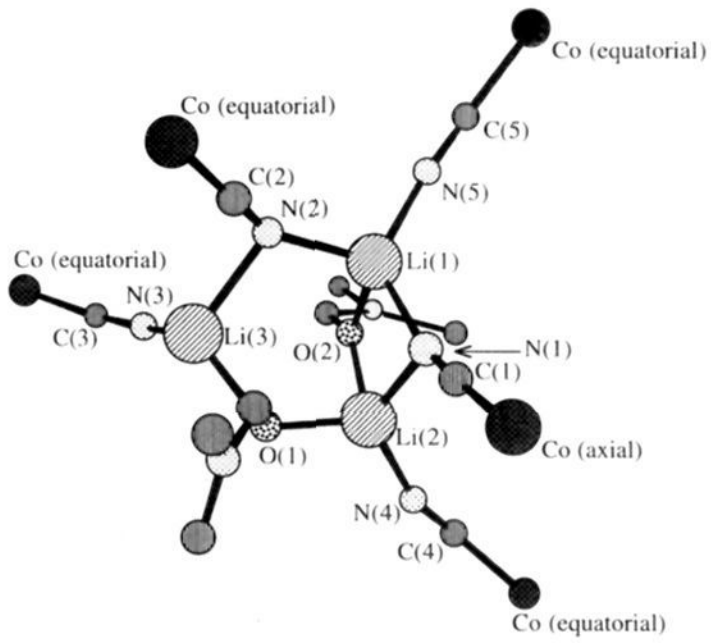

Figure 8. Lithium coordination sphere of **2**.

and an increase in symmetry. Viewed down the b axis, the $Co(CN)_5$ units appear in columns, surrounded by DMF molecules and linked by Li atoms. As in **1**, the structure is an infinite network of $Co(CN)_5$ moieties linked by Li atoms; however, in **2**, all three Li atoms are now closely spaced (Figure 8). All five cyanide ligands and both DMF molecules are bound to the Li atoms. Despite having only seven atoms available to coordinate three Li atoms, Li(1) and Li(2) have approximate tetrahedral, 4-fold coordination and Li(3) has approximate trigonal coordination. This requires a sharing of ligands: two cyanide N atoms and both formyl O atoms bridge two Li atoms. Selected interatomic distances and angles are provided in Table 5, and the positional parameters are given in Table 6.

Examination of a space-filling representation of the structure shows that the DMF molecules have room to move. This likely accounts for the DMF molecules having thermal parameters significantly larger than those of the rest of the structure due to

Table 5. Selected Intermolecular Distances (Å) and Angles (deg) for **2**[a]

Li(1)−N(1)	2.067(33)	Li(1)−N(2)	2.080(34)
Li(1)−N(5)	2.073(33)	Li(1)−O(2)	2.03(4)
Li(2)−N(1)	1.962(34)	Li(2)−N(4)	2.086(32)
Li(2)−O(1)	1.86(4)	Li(2)−O(2)	2.04(4)
Li(3)−N(2)	2.075(34)	Li(3)−N(3)	1.982(34)
Li(3)−O(1)	1.84(4)		
N(1)−Li(1)−N(2)	109.6(17)	N(1)−Li(1)−N(5)	137.7(18)
N(1)−Li(1)−O(2)	89.9(15)	N(2)−Li(1)−N(5)	110.3(17)
N(2)−Li(1)−O(2)	97.2(17)	N(5)−Li(1)−O(2)	98.7(17)
N(1)−Li(2)−N(4)	122.2(19)	N(1)−Li(2)−O(1)	110.1(18)
N(1)−Li(2)−O(2)	92.4(17)	N(4)−Li(2)−O(1)	125.2(20)
N(4)−Li(2)−O(2)	93.1(17)	O(1)−Li(2)−O(2)	100.3(19)
N(2)−Li(3)−N(3)	123.0(20)	N(2)−Li(3)−O(1)	114.4(19)
Li(1)−Li(2)	2.76(5)	Li(1)−Li(3)	2.91(6)
Co(1)−Co(1)	7.340(8), 7.425(8), 7.646(7), 8.4217(4), 9.887(8), 9.951(7), 10.001(7), 10.0846(20), 11.347(4), 11.4579(18)		

[a] Note that intramolecular distances and angles are idealized and have not been refined (C−N, 1.15 Å; Co−C_{axial}, 2.00 Å; Co−$C_{equatorial}$, 1.90 Å; C_{axial}−Co−$C_{equatorial}$, 95.0°).

Table 6. Fractional Coordinates of Non-Hydrogen Atoms for $Li_3Co(CN)_5 \cdot 2DMF$ (**2**)[a]

atom label	X	Y	Z
Co	0.45544(27)	0.9047(5)	0.74184(27)
C1	0.3987(5)	1.0836(7)	0.6637(5)
C2	0.3716(5)	0.8998(11)	0.8284(4)
C3	0.5277(4)	1.0373(9)	0.8279(4)
C4	0.54872(33)	0.8799(11)	0.6682(5)
C5	0.3925(5)	0.7424(7)	0.6687(6)
N1	0.3661(8)	1.1865(10)	0.6187(7)
N2	0.3208(6)	0.8968(17)	0.8808(6)
N3	0.5715(6)	1.1175(14)	0.8800(6)
N4	0.6052(4)	0.8650(17)	0.6237(7)
N5	0.3544(8)	0.6443(11)	0.6244(8)
N6	−0.1422(7)	0.1030(16)	0.4441(7)
C6	−0.1209(13)	0.1590(27)	0.3509(10)
C7	−0.1218(15)	0.2011(19)	0.5313(11)
C8	−0.1809(9)	−0.0400(17)	0.4486(9)
O1	−0.2006(10)	−0.0946(20)	0.5237(12)
N7	0.1573(7)	0.0854(15)	0.1348(7)
C9	0.1860(14)	0.2167(22)	0.2011(14)
C10	0.0640(7)	0.0393(26)	0.1148(16)
C11	0.2180(7)	0.0075(20)	0.0924(10)
O2	0.1991(13)	−0.1032(22)	0.0363(11)
Li(1)	0.3119(23)	0.411(4)	0.6079(28)
Li(2)	0.3165(24)	0.158(5)	0.4847(25)
Li(3)	0.159(4)	0.298(6)	0.4837(27)

[a] Isotropic temperature parameters (U_{iso}, Å^2) are 0.0221(32) for Co, 0.062(8) for C1−C5, 0.034(6) for N1−N5, 0.091(7) for N6−O1, 0.132(8) for N7−O2, and 0.05(18) for Li1−Li3.

either static or dynamic disorder. There is a single microscopic void of sufficient size to accommodate a sphere of diameter 2.8 Å. It is located on an inversion center, between pairs of $Co(CN)_5$ and DMF groups. This void is adjacent to the axial cyanide ligand rather than near the uncoordinated Co site. The void is isolated; thus, the structure demonstrates no microporosity. There is also a smaller void adjacent to the uncoordinated Co site. Visualization shows that dioxygen can be accommodated here with only minor structural reorganization.

O_2 Transport Mechanism in Solids. The X-ray powder patterns of compounds **1** and **2** were measured before and after oxygenation in order to ascertain if any major structural change had occurred. In Figure 9 is shown the powder patterns of **1** under argon and under O_2. It is apparent that the approximate locations of the diffraction lines have not moved although the intensities have changed somewhat. These results show that the crystal lattice does not change appreciably during oxygenation.[17] A similar result was obtained for compound **2**. It

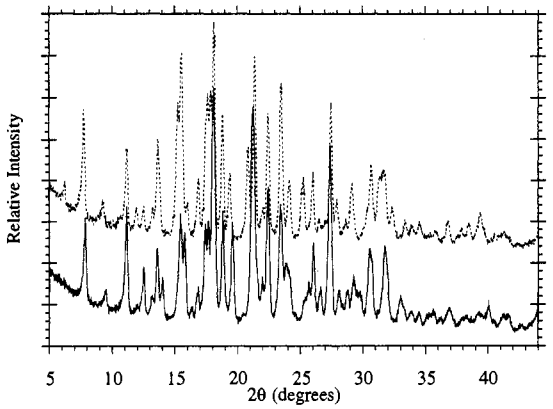

Figure 9. X-ray powder patterns of **1** under Ar (solid line) and under an O_2 (dashed line) atmosphere.

therefore follows that for both compounds **1** and **2** there is enough space in the lattice to accommodate a chemically bound O_2 to each cobalt atom. Indeed, this becomes even more evident when we consider that in both compounds **1** and **2** we reach nearly stoichiometric O_2 capacity, though it takes 600 min for compound **1** compared to 10 min for **2**.

Despite the fact that their lattice can accommodate O_2, compounds **1** and **2** are not porous to other gases such as helium and N_2. This is shown by the agreement between the crystallographically determined density and those measured by helium pycnometry. We must also conclude that O_2 reacts at the surface of the solid and then diffuses to the interior driven by the gradient in chemical potential.

One possible explanation of the much faster oxygenation and deoxygenation rates for **2** vis-à-vis **1** may lie in the sorbents' morphologies. The scanning electron micrographs of **1** and **2** are shown in Figure 10. Crystals of **1** are thin platelets. Upon recrystallization to give **2**, the overall shape of **1** remains, but there are now voids visible in the platelets. Consistent with the appearance of these holes, the BET surface area increases from 5 to >10 m^2/g. Consistent with these results, the low-temperature N_2 adsorption isotherm also reveals the appearance of mesopores with a median diameter of ~300 Å. This phenomenon could also be viewed as a reduction in the effective particle size, leading to a shorter diffusion path length and hence faster rates of O_2 transport.

Experimental Section

General Methods. All chemical synthesis and O_2 sorbent operations were performed using standard Schlenk line or inert atmosphere drybox techniques. Reaction solvents such as DMF and diethyl ether were purchased from Aldrich Chemicals as "sure seal" reagents and used as received. Thermogravimetric analysis (TGA) experiments were carried out using Perkin-Elmer TGS2 and TA 2950 instruments, which were equipped to perform measurements in either an O_2 or N_2 atmosphere. Infrared spectra were taken using a Nicolet 510 FTIR spectrometer. All Raman spectra were obtained with an ISA S-3000 Raman spectrometer with a multichannel detector and microscope sampling accessory. UV−vis spectra were recorded with a Beckman DU-70 spectrophotometer. Routine X-ray powder diffraction measurements were made with a Siemens D-500 powder diffractometer equipped with a diffracted-beam graphite monochromator and controlled-atmosphere cell supplied by Blake Industries.

(17) Unit-cell parameters refined from powder patterns for **1** measured under Ar (*a*, 11.660(4); *b*, 14.324(10); *c*, 8.225(7); α, 96.91(8); β, 103.92(6); γ, 94.37(7)) are quite similar to those measured under O_2 (*a*, 11.793(11); *b*, 14.388(12); *c*, 8.199(6); α, 97.28(8); β, 102.47(11); γ, 95.83(11)). Those for **2** under Ar are the following: *a*, 14.455(4); *b*, 8.423(2); *c*, 14.160(3); β, 97.8(10)). Those for **2** under O_2 are the following: *a*, 14.353(14); *b*, 8.510(7); *c*, 14.102(9); β, 97.6(25)).

The O_2 isotherm measurements were measured on a static volumetric apparatus with the sample immersed in a thermostat bath. The pressure was measured with a capacitance transducer having an accuracy of ±0.15%. The samples were evacuated overnight at ambient temperature prior to analysis.

Preparation of $Li_3Co(CN)_5$·4DMF (1). The procedure described in this section is similar to that used by Carter et al. to prepare what was described as $Li_3Co(CN)_5$·3DMF.[9] Anhydrous cobalt chloride (1.25 g, 9.6 mmol) (Aldrich) was dissolved in 30 mL of DMF with warming. This solution was degassed and then cannula-transferred to a flask containing 150 mL of 0.5 M (50 mmol) LiCN in DMF (Aldrich 0.5 M solution, used as received). The resultant green solution was cooled to 10 °C and kept overnight at this temperature. Green crystals formed at the bottom of the flask. The supernatant solution was removed via a cannula and was discarded. A 30 mL portion of diethyl ether was added to the product by cannula and was then removed immediately via another cannula. The solid was dried in vacuum (0.003 Torr) for 2 h at room temperature. A pale green solid interspersed with dark green chunks was collected. The yield of **1** was 2.63 g. An elemental analysis of one preparation of this compound gave a best fit with the formula $Li_3Co(CN)_5$·5DMF. Anal. ($C_{20}H_{35}CoLi_3N_{10}O_5$) C, H, Li, Co; N: calcd, 24.35; found, 23.58. We believe that the extra molecule of DMF is weakly absorbed residual solvent.

The amount of DMF in **1** varies with preparative conditions. For instance, in a slight modification of the above synthesis, the $CoCl_2$ solution was added to the LiCN solution with vigorous stirring to precipitate a green powder. This was filtered, washed with large amounts of ether, and dried in vacuum at 25 °C for 2 days. The light green powder was found by elemental analysis to have the formula $Li_3Co(CN)_5$·3.5DMF. Satisfactory analytical data (±0.4% for Co and Li) were obtained. We infer that washing **1** repeatedly with ether followed by rigorous drying can dislodge some DMF.

Compound **1** tends to precipitate from the reaction mixture as a fine powder, and attempts to recrystallize it failed. For an X-ray structural determination, very small single crystals were grown by the slow addition of a 0.125 M cobalt chloride solution in DMF to a 0.25 M solution of LiCN also in DMF to a final total Co^{2+}:CN molar ratio of 1:5.2. The crystals were filtered and collected under a N_2 atmosphere. A powder diffraction pattern calculated from the single-crystal results closely matched that measured for the powder, confirming that the crystal selected was representative of the bulk (see Figure S1 in the supporting information).

The infrared spectra in the cyanide region [2104 (s), 2125 (m) cm^{-1}] of our samples are similar to those reported by Carter et al. [2097 (s), 2127 (m) cm^{-1}] of stated formula $Li_3Co(CN)_5$·3DMF.

Preparation of $Li_3Co(CN)_5$·2DMF (2). A sample of **1** that analyzed as $Li_3Co(CN)_5$·5DMF was loaded on the pan of a Perkin-Elmer TGA instrument with a minimum exposure to air. It was heated under a purge of N_2 (100 cm^3/min) at a rate of 5 °C/min to a temperature of 160 °C and held there for 20 min. At temperatures <130 °C, a weight loss of 12.4% was observed, corresponding to evolution of approximately one weakly held DMF molecule. Between 130 and 160 °C, a further 24.81% loss occurred, wherein two tightly held DMF molecules were evolved. This process led to a material with nominal composition $Li_3Co(CN)_5$·2DMF. The same material can be obtained by heating $Li_3Co(CN)_5$·3.5DMF to 160 °C to remove ~1.7 DMF molecules. Anal ($C_{10.4}H_{12.6}CoLi_3N_{6.8}O_{1.8}$) C, H, Li; N: calcd, 27.89; found, 27.43.

Crystal Structure Determination for $Co(CN)_5Li_3$·4DMF (1).[18] A yellow plate-shaped single crystal of **1**, with approximate dimensions 0.25 × 0.15 × 0.07 mm was mounted on a glass fiber. In order to obtain adequate diffraction intensities, a diffractometer with a 12 kW rotating-anode generator was needed. Diffraction data were collected under a flow of N_2 at −120 °C. Unit cell dimensions and an orientation matrix were determined from 23 reflections with 2θ values between 20° and 27°. The crystal structure of complex **1** was solved by direct methods using the SHELXS-86 program,[19] and refinements were conducted in the teXsan Crystal Structure Analysis package.[20,21]

Crystal Structure Determination for $Co(CN)_5Li_3$·2DMF (2). Single crystals of **2** cannot be obtained by simply removing DMF from

(18) Crystal structure solution was performed by Molecular Structure Corp., The Woodlands, TX.

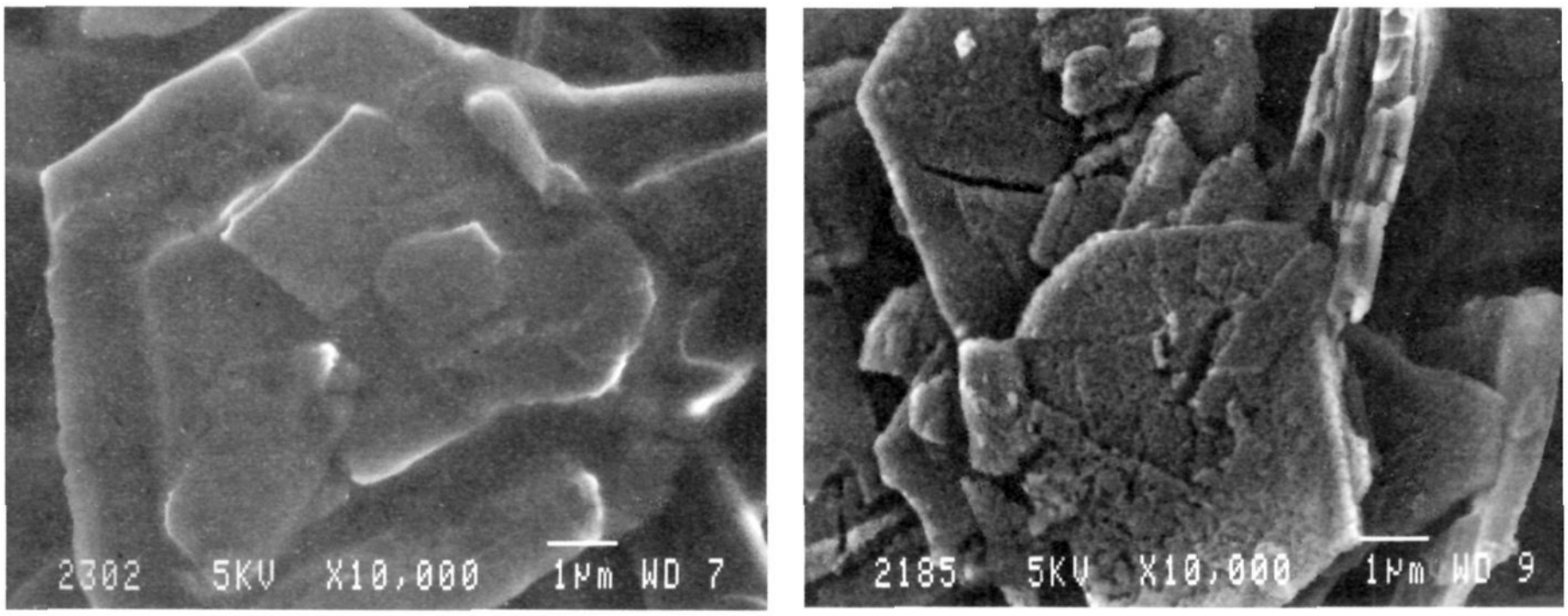

Figure 10. Scanning electron micrographs of **1** (a, left) and **2** (b, right). The white horizontal bars represent 1 μm for scale.

1 by heating, and no other method for producing **2** was found. Attempts were thus made to determine the structure of **2** from powder X-ray diffraction. A sample of **2** was sealed inside a 0.7 mm quartz capillary. Diffraction data were collected by using the X7A X-ray diffractometer at the Brookhaven National Laboratory National Synchrotron Light Source.[22] A wavelength of 1.299 45(2) Å was obtained using a channel-cut Si(111) monochromator crystal and a Ge(220) analyzer crystal. Peak positions for the first 40 diffraction peaks were determined by manual profile fitting and were automatically indexed using program ITO[23] to a monoclinic unit cell. This unit cell was checked using the NIST*LATTICE program[24] to search for higher symmetry unit cells and for cells that could be related to the triclinic unit cell of complex **1**. Neither attempt was successful. The highest symmetry space group consistent with the observed diffraction pattern was $P2_1/n$. A Patterson map was computed from intensities extracted using the Le Bail method.[25] No internally consistent assignment could be made for the heavy atom site from this map, presumably due to the high degree of overlap and the small intensities observed at high angles. It was anticipated that direct method solution attempts would suffer from the same problems.

On the basis of the unit cell dimensions, density, chemical analysis, and spectroscopic results, and assuming the highest symmetry space group consistent with systematic extinctions, the asymmetric unit can be presumed to contain a single $Co(CN)_5$ unit and two DMF molecules. Using this information, the structure was solved using a rigid-body simulated annealing technique, similar to that described by Harris, *et al.*[26] Using a customized script within the Biosym Technologies Catalysis and Sorption package,[27] a $Co(CN)_5^{3-}$ and two DMF moieties were placed at random positions in a unit cell of appropriate dimensions. Crystallographic symmetry was used to generate the unit cell contents. Translations and rotations were then applied randomly to each of the three moieties according to a Metropolis Monte Carlo algorithm[28] where the agreement between the observed and computed diffraction data was used to select or reject these steps. Starting from different random positions, approximately 20 different Monte Carlo runs were made. These runs produced several models with agreement factors (R_{wp}) in the range of 0.25−0.3 which were then refined using the GSAS Rietveld package.[29,30]

For the Rietveld refinements, the $Co(CN)_5^{3-}$ moiety was constrained to C_{4v} symmetry with bond distances and angles (given in Table 5) approximating those of the $Co(CN)_5^{3-}$ moiety of **1**. The two independent DMF molecules were constrained to an idealized geometry generated by using the "cvff" force field in DISCOVER.[27] A rigid-body (group) refinement was used to optimize the orientations of these three moieties. Thus, the $Co(CN)_5^{3-}$ and DMF intramolecular distances and angles were not optimized during the refinement, and the hydrogen atom positions were assumed rather than directly observed.

The best trial model obtained from the Monte Carlo procedure converged with a R_{wp} value of 0.18. This model was then improved by manually rotating the DMF molecules to better fit difference Fourier maps: in these orientations the O atoms were oriented toward cyanide N atoms. Further refinements, with addition of grouped temperature factors, allowed R_{wp} to drop to 0.11. A subsequent difference Fourier map exhibited two peaks with approximate tetrahedral coordination by formyl O and cyanide N atoms. These peaks were assigned as Li(1) and Li(2). The refinement was continued, placing "soft constraints" on the Li−N and Li−O bond lengths of 2.0(1) Å. A subsequent Fourier map showed a broad peak consistent with approximate 3-fold coordination. This peak was assigned as the final Li(3) atom, and soft constraints of 2.0(1) Å were also applied to these three bonds. Temperature factors were refined by grouping chemically similar atoms. In the final stages of refinement, the weighting of soft constraints was lowered to a point where the contribution of the soft constraints to the total χ^2 is less than 1%. Further reduction in this weighting factor resulted in unrealistic Li bonding distances, and did not produce a

(19) Sheldrick, G. M. SHELXS-86. A program for the solution of crystal structures from diffraction data, Institute für Anorganische Chemie der Universitat, Tammannstrasse 4, Gottingen, Germany.

(20) TEXSAN Structure Analysis Package, Molecular Structure Corp., 1985.

(21) The single-crystal structure of **1** was refined to minimize $\sum w(|F_o| - |F_c|)^2$ using $w = 4F_o^2/\sigma^2$ and $\sigma^2 = [S^2(C + R^2B) + (0.03F_o^2)^2]/Lp^2$ where S is the scan rate, C is the total integrated peak count, B is the total integrated background count, R is the ratio of scan times for the peak scan to the background, and Lp is the Lorentz polarization correction. Weighted and unweighted R factors are defined as $R_w = [[\sum w(|F_o| - |F_c|)^2]/\sum wF_o^2]^{1/2}$ and $R = [\sum||F_o| - |F_c||]/\sum|F_o|$.

(22) Cox, D. E.; Toby, B. H.; Eddy, M. M. *Aust. J. Phys.* **1988**, *41*, 117.

(23) Visser, J. W. *J. Appl. Crystallogr.* **1969**, *2*, 89.

(24) Karen, V. L.; Mighel, A. NIST*LATTICE. NIST Technical Note 1290; National Institute for Standards and Technology: Gaithersberg, MD, 1991.

(25) Le Bail, A.; Duroy, H.; Fourquet, J. L. *Mater. Res. Bull.* **1988**, *23*, 447.

(26) Harris, K. D. M.; Tremayne, M.; Lightfoot, P.; Bruce, P. G. *J. Am. Chem. Soc.* **1994**, *116*, 3543.

(27) Catalysis and Sorption Consortium Software, Biosym Technologies, Inc., San Diego, CA.

(28) Metropolis, N.; Rosenbluth, A. W.; Rosenbluth, M. N.; Teller, A. H.; Teller, E. *J. Chem. Phys.* **1953**, *21*, 1087.

(29) Larson, A. C.; Von Dreele, R. B. GSAS, Generalized Structure Analysis System. Report LAUR 86-748; Los Alamos National Laboratory: Los Alamos, NM, 1988.

(30) Rietveld refinement was used to minimize $\sum w_i(I_{o,i} - I_{c,i})^2$ for **2** where $I_{o,i}$ and $I_{c,i}$ are the observed and calculated powder diffraction intensities for the ith point, respectively. Weights, w_i, are $1/I_{o,i}$. Weighted and unweighted profile R factors are defined as $R_{wp} = [[\sum w_i(I_{o,i} - I_{c,i})^2]/\omega w_i I_{o,i}^2]^{1/2}$ and $R_p = [\sum|I_{o,i} - I_{c,i}|]/\sum I_{o,i}$. The expected R factor (the statistically best possible value for R_{wp}) is defined as $R_c = [[N - P]/\sum w_i I_{o,r}^2]^{1/2}$ where N is the number of observed powder diffraction data points and P is the number of refined parameters. The Bragg R factor, R_B, is defined as $R_B = [\sum||F_o| - |F_c||]/\sum|F_o|$, using estimated values for the observed structure factors, F_o.

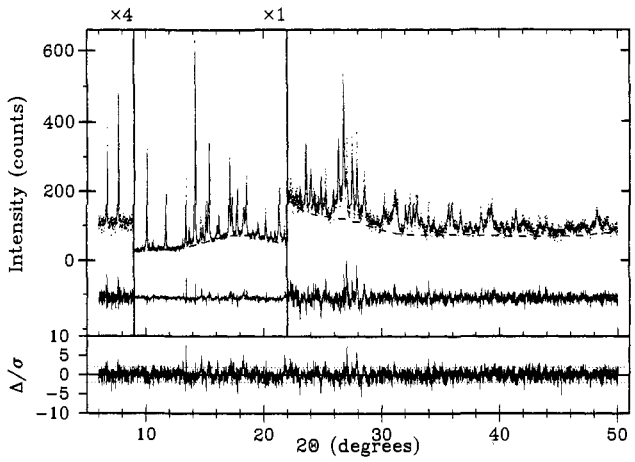

Figure 11. Observed diffraction pattern (dots) overlaid with a pattern calculated from the crystal structure (solid line) and the fitted background (dashed line). Reflection positions are noted by vertical lines. Deviations between the observed and calculated intensities are shown below on the same scale as the observed pattern. The lower box shows the same deviations relative to the estimated standard deviation for each point; a dashed line is drawn at $\pm 2\sigma$. Note that sections of the upper plot are magnified to improve clarity. A scale factor is noted above the upper box.

significant improvement in R factors. The low sensitivity of the reffinement to Li siting is expected due to the small scattering power of this element.

Considering the use of a highly constrained model, the agreement between the observed and computed diffractograms, shown in Figure 11, is spectacular. This is also noted by the closeness of the ratio of the weighted profile R factor (R_{wp}) to the statistically expected agreement factor (R_e) to unity. Thus, addition of more parameters to the refinement would not provide a more accurate structural model, since the data do not provide a sufficient number of independent observations. For this reason, no attempt was made to refine individual atomic positions. While the structure cannot reveal all of the details of intramolecular bonding, the excellent agreement between the model and observations and the highly plausible chemical model indicates that it is a very reliable representation of the packing structure of **2**.

Conclusions

It has long been recognized that pentacyanocobaltate(3−) salts irreversibly bind dioxygen. We have found that, quite remarkably, the lithium pentacyanocobaltates **1** and **2** ($Li_3[Co(CN)_5]\cdot x$DMF, $x = 4$, 2, respectively) reversibly bind O_2. Under ambient conditions, **1** and **2** can absorb close to one molecule of O_2 per molecule Co and the gas can be readily released by decreasing the partial pressure of O_2. Dioxygen uptake and release are much faster for the lower solvate compound, **2**, which shows an unprecedented equilibrium O_2 capacity. Structural studies have shown that both compounds are extended solids with DMF-bound Li cations cross-linking $Co(CN)_5^{3-}$ units through the cyanide N atoms. We hypothesize that the reversibility in O_2 binding results from decreased electron density on Co due to the Lewis acidity of the interconnecting Li ions.

Crystals of **1** and **2** are dense solids for which there is no indication of microporosity. The observed facile access of dioxygen into crystals of **2** is believed to be a function of the material's morphology (see Figure 9) and occurs by a chemical reaction driven, solid state diffusion mechanism.

Acknowledgment. We would like to acknowledge the Biosym Technologies Catalysis and Sorption Consortium, with particular thanks to Clive Freeman, for help in the development of the rigid-body simulated annealing software that was used to solve the structure of **2**. We are also grateful to David Cox of Brookhaven National Laboratory for access to the synchrotron X-ray diffractometer. Work at the National Synchrotron Light Source is supported by the U.S. Department of Energy, Departments of Materials Sciences and Chemicals Sciences. The expert analytical services of Gary Johnson, James Stets, Fred Lucrezi, and J. Douglas Moyer, Jr., are gratefully acknowledged.

Supporting Information Available: Details of the X-ray structure determination for **1**, tables of atomic coordinates, atomic displacement parameters, bond lengths, bond angles, torsion angles, nonbonded contacts and selected least-squares planes for **1**, Table SI containing H atom coordinates for **2**, and Figure S1 showing calculated and observed powder diffraction patterns for **1** (25 pages); a listing of observed and calculated structure factors for **1** (10 pages). This material is contained in many libraries on microfiche, immediately follows this article in the microfilm version of the journal, can be ordered from ACS, and can be downloaded from the Internet; see any current masthead page for ordering information and Internet access instructions.

JA951406S